Soft-Template Synthesis and Characterization of ZnO2 and ZnO Hollow Spheres

ARTICLE *in* THE JOURNAL OF PHYSICAL CHEMISTRY C · JULY 2009

Impact Factor: 4.77 · DOI: 10.1021/jp9036028

Soft-Template Synthesis and Characterization of ZnO_2 and ZnO Hollow Spheres

S. Cheng,[†] D. Yan,[†] J. T. Chen,[†] R. F. Zhuo,[†] J. J. Feng,[†] H. J. Li,[†] H. T. Feng,[†] and P. X. Yan*[,†,‡]

School of Physical Science and Technology, Lanzhou University, Lanzhou 730000, People's Republic of China, and Key Laboratory of Solid Lubrication, Institute of Chemistry and Physics, Chinese Academy of Science, Lanzhou 730000, People's Republic of China

Received: April 13, 2009; Revised Manuscript Received: June 4, 2009

Zinc peroxide (ZnO_2) hollow spheres of 100−200 nm diameter were synthesized by a simple hydrothermal method by using H_2O_2 and ZnO powder as reagents without the assistance of any surfactant. O_2 bubbles in situ generated by the decomposition of H_2O_2 served as a soft template in the formation of ZnO_2 spheres. Zinc oxide (ZnO) hollow spheres were obtained by heat treatment of ZnO_2 hollow spheres at 180 °C for 10 h in air. The products were characterized by XRD, FT-IR, TEM, HRTEM, and FESEM. The transition temperature of ZnO_2 to ZnO was determined to be 229 °C by TG-DTA. Photoluminescence (PL) properties of the products were investigated and the origin of the two peaks at 392 and 448 nm in the PL spectrum of ZnO_2 was discussed. Furthermore, the growth mechanism of the ZnO_2 hollow spheres was discussed in detail.

Introduction

Recently, hollow micro/nanostructures have become of great interest because of their excellent characteristics such as low density, high surface-to-volume ratio, and low coefficients of thermal expansion and refractive index, which makes them attractive for applications ranging from catalyst support, antireflection surface coatings, microwave absorption,[1,2] encapsulating sensitive materials,[3,4] drug delivery,[1,2] and rechargeable batteries.[1,5,6] Rapid developments in the synthesis of hollow structures, such as CuO,[7,8] Cu_2O,[9,10] TiO_2,[11,12] SnO_2,[13−15] Fe_2O_3,[8] Co_3O_4,[16,17] β-$Ni(OH)_2$,[18] α-MnO_2,[19] CuS,[20−22] Sb_2S_3,[23] ZnO,[24,25] $CdMoO_4$,[26,27] and $ZnWO_4$,[28] have greatly advanced our ability to tune their mechanical, optical, electrical, and chemical properties to satisfy the various needs of practical applications. ZnO_2 can be useful in many fields, such as in the rubber industry,[29−31] photocatalysis,[32] synthesis of ZnO,[32−34] cosmetic and pharmaceutical industries, and for therapeutic applications,[35] but little work have been done in these areas.[35−37] ZnO, as a wide gap semiconductor material, is becoming an increasing concern because of its biocompatibility, nontoxicity, and good mechanical, optical, electrical properties. Thus, research about ZnO_2 and ZnO hollow spheres is of great importance and should be paid more attention.

The thermal evaporation process and the hydrothermal method were commonly used to synthesize ZnO hollow microspheres.[24,25,38−45] However, the thermal evaporation process always faces disadvantages related to requiring special equipment, high temperatures (typically >500 °C), and vacuum conditions. The hydrothermal synthesis of ZnO hollow spheres usually involves a template-assisted process, such as conventional hard templating synthesis, sacrificial templating synthesis, and soft templating synthesis, which makes the synthesis process complicated and further treatments to remove the template are often required. Moreover, the size of the products is usually on the order of micrometer or even larger. Therefore, the synthesis of ZnO_2/ZnO hollow spheres with diameters of submicrometer and nanometer size by a simple and efficient method is of significant importance and it is still a great challenge for researchers.

In this work, we developed a simple hydrothermal synthesis with a high yield (nearly 100%) of ZnO_2 hollow spheres, using H_2O_2 and ZnO powder as reactants, without the assistance of any conventional hard templates, which made the synthesis process more efficient. Interestingly, the O_2 bubbles in situ generated by the decomposition of H_2O_2 acted as both an important intermediate oxidizer and a special soft template, which is crucial to the formation of ZnO_2 hollow spheres. The as-produced samples can easily convert to ZnO hollow spheres by simple heat treatment in air at 180 °C for 10 h. Furthermore, the PL properties of the products were investigated and the growth mechanism of the hollow spheres was discussed in detail.

Experimental Details

All chemicals used are analytical pure grade and were used without further purification. In a typical procedure, 5 mL of distilled water and 400 mg of ZnO powder were put into a glass beaker and ultrasonically dispersed to obtain a uniform mixture. Then 25 mL of 30% (wt %) hydrogen peroxide (H_2O_2) aqueous solution was added and the resulting mixture was transferred into a Teflon-lined autoclave (45 mL), tightly sealed, and treated at 150 °C for 20 h. Then the autoclave was cooled to room temperature naturally and the precipitates were finally dried at 60 °C in air without washing. ZnO hollow spheres were obtained by heat treatment of the ZnO_2 hollow spheres at 180 °C for 10 h in air.

The products were characterized by X-ray diffraction (XRD) on a Rigaku D/Max-2400 and a Philips X' Pert Pro Diffractometer, using Cu $K\alpha_1$ radiation ($\lambda = 1.54056$ Å). Morphology of the samples was investigated by field emission scanning electron microscopy (FESEM) on a Hitachi S-4800 and a JSM 6701F field emission scanning electron microscopy. Transmission electron microscopy (TEM) observation and selected area electron diffraction (SAED) were performed on a Hitachi H-600 transmission electron microscopy operated at 100 kV, and

* To whom correspondence should be addressed. E-mail: pxyan@lzu.edu.cn. Phone:86+0931+8912719. Fax: 86+0931+8913554.
[†] Lanzhou University.
[‡] Chinese Academy of Science.

10.1021/jp9036028 CCC: $40.75
Published on Web 07/07/2009

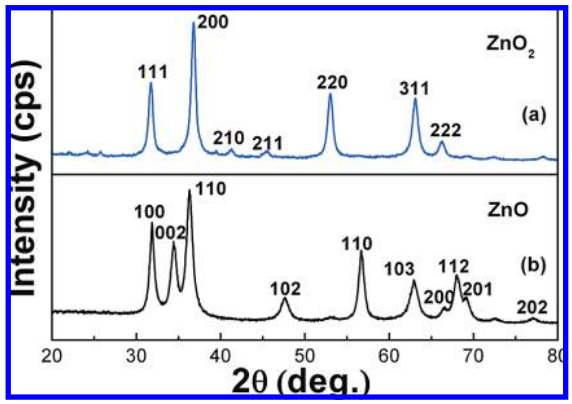

Figure 1. XRD patterns of ZnO_2 and ZnO: (a) hollow ZnO_2 nanospheres obtained through the hydrothermal method at 150 °C and (b) hollow ZnO nanospheres obtained by the calcination of ZnO_2 at 180 °C for 10 h.

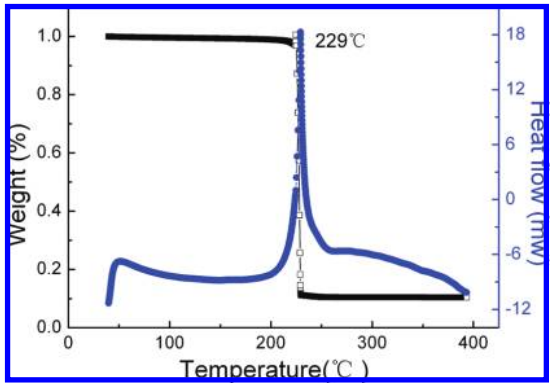

Figure 2. TGA-DSC curves for ZnO_2.

HRTEM were carried out on a TECNAI F30 high-resolution transmission electron microscopy. Fourier transform infrared (FT-IR, Bruker IFS66 V/S) spectra were recorded for the flakes of samples pressed with KBr powder, which was dried at 70 °C to eliminate the effect of water molecules. The room temperature photoluminescence (PL) spectrum of ZnO_2 was recorded on a fluorescence spectrophotometer (FLS920 T) by using the 325 nm line as the exciting source. The thermogravimetry/differential thermal analyzers (on TG-DTA 6300) analysis of the as-synthesized products was also carried out.

Results and Discussion

Structure Analysis. The XRD patterns of the as-synthesized products (Figure 1a) and the samples after heat treatment (Figure 1b) were shown in Figure 1. Figure 1a reveals the crystal structure and phase purity of the ZnO_2 nanostructures. The entire diffraction peaks match well with the cubic structure ZnO_2 (JCPDS card No. 13-0311). Figure 1b shows that the sample after thermal treatment is wurtzite ZnO (JCPDS card No. 36-1451). Therefore, it can be concluded that the as-prepared sample was ZnO_2 and the product after heat treatment is ZnO.

Figure 2 reveals an exothermic peak (~229 °C) for oxygen release, according to the following reaction:

$$ZnO_2(s) \rightarrow ZnO(s) + 2O_2(g) \quad (1)$$

The temperature of the oxygen release (~229 °C) is in accord with the value from the literature.[35,36,48] According to the curve, the weight loss was 89.5%. This value is much larger than 16.4%, which is the weight loss of O_2 when ZnO_2 was completely decomposed into ZnO. In the experiment, it is observed that a large amount of solid powder was entrained out of the opened porcelain boat and only a little light yellow powder was left after high-temperature thermal treatment. And the weight loss are almost the same at each heat treatment process, which was identified by another TG-DTA measurement, and that was about 84.5% (not shown). As far as we know, part of the ZnO powder was carried out of the porcelain boat along with the decomposition of the ZnO_2 and the release of O_2, because the hollow sphere structure broke into very small nanoparticles (a few nanometers) instantly and they can be entrained away by the O_2 and N_2 (the protect atmosphere) easily. Also the hollow sphere structure would be introduced, as shown in detail at the following text.

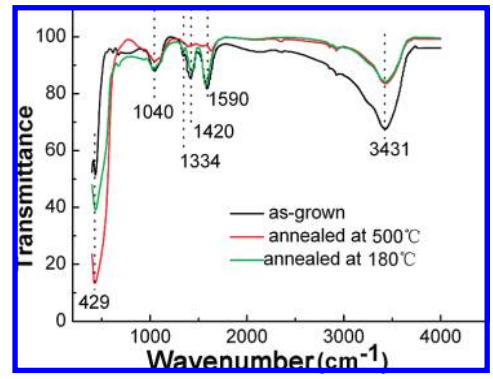

Figure 3. FTIR spectrum of the (a) as-grown and annealed samples (b) at 180 °C (c) at 500 °C.

Figure 3 shows the FTIR spectra of the samples of as-grown (ZnO_2), annealed at 180 °C (ZnO) and 500 °C (ZnO). The absorption peaks at about 3431 and 1590 cm^{-1} are attributed to the stretching vibration of the O−H bond and the bending vibration of H−O−H from water molecules, respectively. Another sharp absorption band of the samples is observed located at 429 cm^{-1}. The peak positions of both ZnO_2 and ZnO are the same, but with a little different in bandwidth, which is because of the different adjacent valences, corresponding to Zn−O vibration band, which is consistent with previous reports.[49,50] The peak positions centered at 1040, 1334, and 1420 cm^{-1} should relate to the O_2^{2-} ions and may arise from the O−O bands, because ZnO prepared by low-temperature heat treatment of the ZnO_2 may contain some O_2^{2-} ions.[47]

Morphology Analysis. Figure 4 shows the FE-SEM images of the as-prepared product ZnO_2 and the ZnO (180 °C annealing product). Figure 4a is an overview of the as-prepared sample. Obviously, the product is composed of submicrospheres with diameters of 100−200 nm. It can be found that the sphere indicated by the arrow is opened and may be broken in the synthesis process. Figure 4b is the high-magnification image. The diameters of the spheres are about 100−200 nm as seen from Figure 4b. The shell thickness of the hollow submicrospheres is about several tens of nanometers and the shells are composed of small nanoparticles, which can be seen more clearly from the HR-TEM images. The morphology of the sample annealed at 180 °C does not have an obvious change because of the sufficiently low decomposition temperature, as shown in Figure 4, panels c and d. And the diameters of the ZnO spheres remain the same as those of the as-obtained product ZnO_2. Some spheres are much bigger and may be formed by several adjacent small spheres joined together when the sample was heated in air atmosphere, such as the big opened sphere shown by the arrow in Figure 4c. And Figure 4d is the high-magnification image of the same sample.

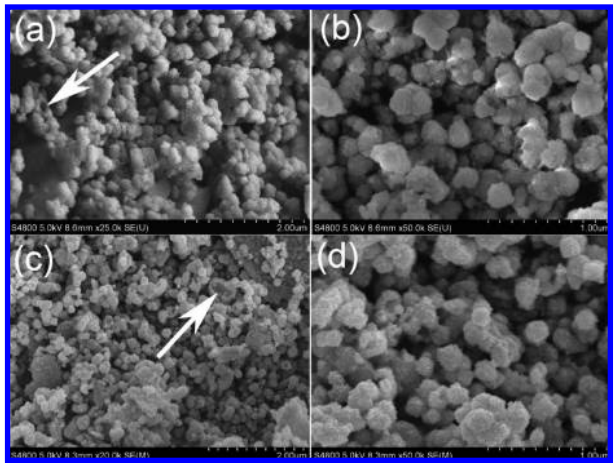

Figure 4. (a) Low- and (b) high-magnification FE-SEM images of hollow microspheres of the as-obtained product, ZnO_2, and (c) low- (d) high-magnification FE-SEM images of the anealing product ZnO, anealed at 180 °C

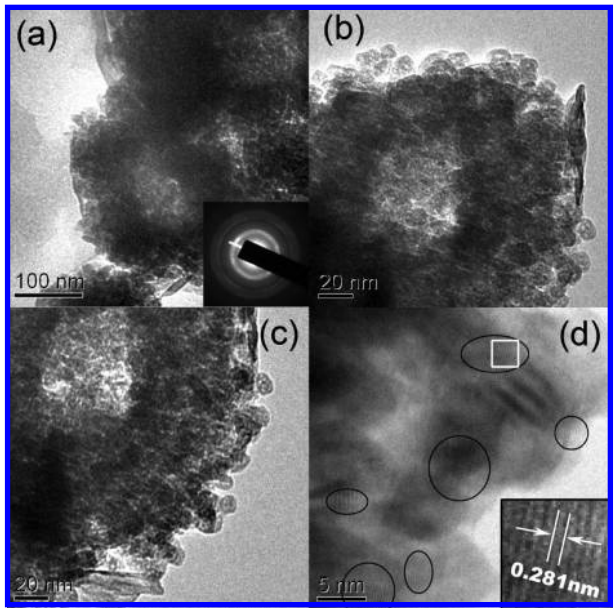

Figure 5. HR-TEM images of the as-obtained product ZnO_2. (a) Low- and (b, c) high-magnification images of one sphere. (d) Atomic structure, confirming a cubic structure with lattice fringe 2.81 Å of the (111) plane. The inset of panel a is the SAED pattern.

Further insight into the morphology and microstructure of the as-obtained product ZnO_2 was gained by using HR-TEM, indicated in Figure 5. The view of one sphere (Figure 5a) shows the product is a hollow structure whose shell is composed of uniform nanoparticles that may also be hollow structures with diameters of several nanometers, and Figure 5b clearly reveals this structure and the spheres' diameters are around 200 nm, and the shell thickness is about 60 nm, which agrees with the FE-SEM images. Details of the hollow structures were demonstrated by a close view of the sample (Figure 5c). The atomic structures of ZnO_2 were also characterized by HR-TEM, as shown in Figure 5d. It shows that the ZnO_2 submicrometer-sized spheres are multicrystalline, with one of the lattice spacings of about 0.281 nm, corresponding to the distance between the (111) planes in the ZnO_2 crystal lattice, which is indicated by the cubic, as shown in the inset of Figure 5d. The selected area electron diffraction (SAED) pattern of the ZnO_2 sample (the inset of Figure 5a) confirms that it is multicrystalline, which is consistent with the image of Figure 5d.

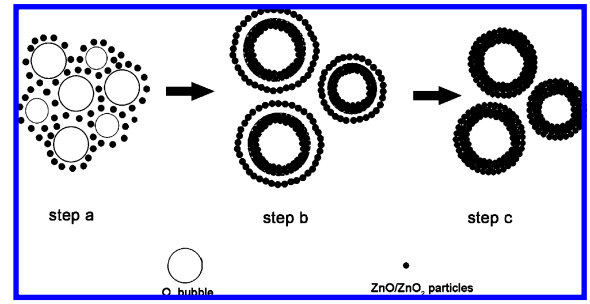

Figure 6. A schematic drawing of the possible formation mechanism of hollow nanospheres: (a) dissolution of the precursor and formation of O_2 gas bubbles and (b−c) formation of ZnO hollow microspheres.

Growth Mechanism. Figure 6 is a schematic illustration of the hollow spheres' growth process. The experimental results indicate that the in situ generated O_2 gas bubbles serve as a soft template during the process of forming hollow spheres.[1,51,52] On the basis of these observations, a mechanism for the formation of ZnO_2 hollow submicrospheres is proposed, with reference to the preparation of monodispersed ZnSe, or ZnO microspheres.[51,52] In our experiments, the precursor of ZnO powder was dispersed into small particles by ultrasonic irradiation, first. So they can be easily dissolved in the solution and formed ZnO monomers in the hydrothermal environment, relatively elevated temperature, and high pressure. As illustrated in Figure 6, after the initial nucleation, the monomers were grown into nanoparticles. These nanoparticles have a tendency to aggregate and many O_2 nanobubbles decomposed by hydrogen peroxide provided the aggregation center (step a). Driven by the minimization of the interfacial energy, small ZnO nanoparticles may aggregate around the gas−liquid interface between O_2 and water, and were finally emerged to hollow ZnO spheres (steps b and c). At the same time, ZnO was oxidized into ZnO_2 by O_2 gas, so the ZnO_2 hollow spheres were finally formed. It appeared that the forming process of hollow ZnO was layer-by-layer (step b), which was identified by the following parallel experiments. The space between layers was full of O_2, which was consumed at the oxidization procedure, and the layers were finally connected together (step c). The in situ generated gas bubbles help the nanoparticles to aggregate and form hollow spheres. But the attachment of solid particles to gas bubbles is a complex process, which is affected by many factors, such as particle surface properties, particle size, electrostatic interactions, and hydrodynamic conditions.[53] At the most important step (step b) for formation of hollow spheres, the existence of larger amounts of O_2 and a gas−liquid equilibrium in the autoclave is the key factor, which makes the formation of gas bubbles a soft template and the hollow products finally. In a word, the morphology is mainly dependent on the concentration of hydrogen peroxide and the amount of ZnO precursor which affect the relative concentration of gas bubbles, and the heat temperatures relating to the decomposition velocity of hydrogen peroxide as well as the reactive time also remarkably affect it, all of which were identified by the parallel experiments.

In the experiments, when we reduced the amount of hydrogen peroxide to 15 mL, the quantity of hollow spheres decreased and rod-like structures appeared, as shown in Figure 7, which is the SEM images of the products, (a) low- and (b) high-magnification images. Hence, we can think that the proper amount of hydrogen peroxide is in favor of the formation of hollow spheres. Moreover, we also varied the amount of ZnO precursor to investigate its effect. At conditions of different ZnO

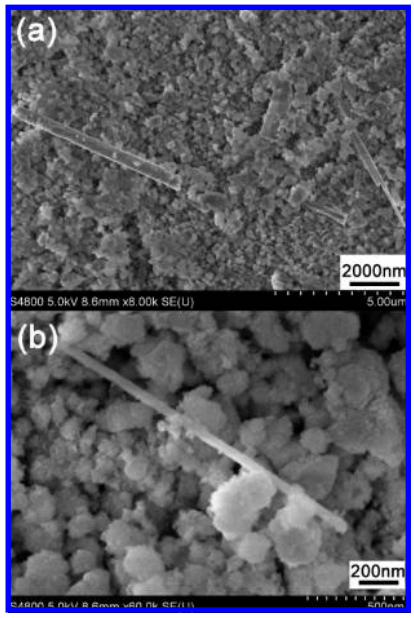

Figure 7. SEM images of the products reacted with 15 mL of H_2O_2: (a) low- and (b) high-magnification images.

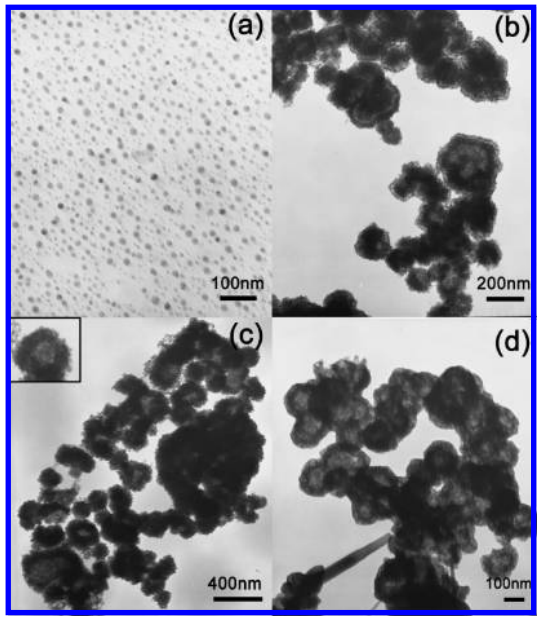

Figure 8. TEM images of the control experiment results: (a) image of the as-obtained product, ZnO_2, reaction time prolonged to 44 h, and (b−d) hollow ZnO_2 microspheres heated at 120, 150, and 180 °C, respectively.

amounts, we obtained different yields of hollow sphere, and they are accompanied by solid sphere, sphere-like agglomeration, the aggregation of nanoparticles, and a few nanorods. So the appropriate amount of ZnO precursor is also an important factor to form a mass of ZnO_2 hollow spheres. And the morphology change derived from the increase of ZnO concentration is similar to that resulting from the reduction of the hydrogen peroxide amounts.

To identify the influence factors of the products' morphologies, a series of control experiments were conducted. Figure 8 indicates the TEM images of the products with different morphologies. When the heating time was prolonged to 44 h, uniform nanoparticles were formed, which is shown in Figure 8a, and their diameters are around several nanometers, which is the same order of magnitude as the nanoparticles composing

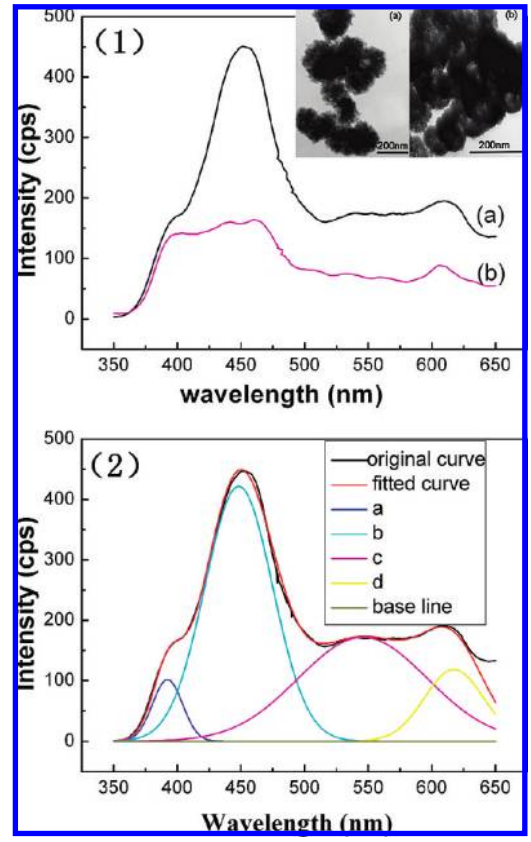

Figure 9. Photoluminescence spectra of as-obtained products with (a) 300 and (b) 400 mg of ZnO as precursor, respectively.

the hollow spheres' shell. When the heating time was longer than 48 h, small superthin nanoflakes were formed (not shown), which is presumed to be the unfolding results of the nanoparticles mentioned above. So we can further conclude that the nanoparticles are hollow, which is in accordant with the HR-TEM results and the TG-DTA results referred to above. To investigate the effect of reactive temperature, we also conducted the temperature-control experiments at 90, 120, 150, and 180 °C, respectively. When the temperature is 90 and 180 °C, the dominant morphology of the product is nanorods and some anomaly spheres exist, as shown in Figure 8d, the TEM image of the products heated at 180 °C, which indicated that the shells of the spheres are composed of a flake-like structure different from the products obtained at 150 °C. Figure 8b is the image of the product heated at 120 °C. The shells are layered, which can be regarded as one of the forming processes of the final hollow sphere products (heated at 150 °C), which is shown in Figure 8c, and the inset is a single magnified one. As we see, temperature can remarkably influence the growth of nanocrystals. And the kinetics of nucleation and growth as well as processes such as coarsening and aggregation are expected to be strongly dependent on the properties of the reaction temperature.

PL Spectra. Figure 9 shows the PL spectra of the as-obtained samples ZnO_2 with reactant ZnO, 300 mg (named sample "a") and 400 mg (named sample "b"), with excitation wavelength of 325 nm. The inset of Figure 9(1) is the features of these two samples. The PL spectra of sample "a" was deconvoluted into four components, which are centered at 392, 448, 545, and 618 nm, as shown in Figure 9(2); the colored curves indicate these peaks, respectively, and the red curve is the fitted one. However, sample "b", formed at the same conditions except for the quantity of the reactant ZnO, exhibits a weak wide emission

band from 400 to 475 nm, which is almost flat in this range, and a weak peak at about 610 nm, as shown in Figure 9(1b). As we know, ZnO_2 is an indirect band semiconductor, the band gap value is between 3.71 eV for the annealed ZnO_2 film and 5.7 eV for the as-grown ZnO_2 film on quartz,[54] which was also calculated by first-principles simulation, and is in the range of 3.3−4.6 eV for ZnO_2 nanoparticles.[36] The intrinsic transition probability for the indirect semiconductor is very small and the un-intrinsic transition plays a main role instead, which is related to the lattice vibration. The shoulder peak of the former one centered at 392 nm should be the band edge emission, which is rather weak. And the green-blue wavelength centered at 448 nm originates from the oxygen vacancy. Sample "b" is a hollow structure and the empty space is full of oxygen, but most of sample "a" is solid and there is not enough oxygen element, as shown in the inset of Figure 9(1). So there is a greater shortage of oxygen in the ZnO_2 cubic structure of sample "a", and the density of the surface oxygen vacancy is higher, oppositely. Hence, the intensity of this peak originating from the oxygen vacancy for sample a is much stronger, as shown in Figure 9(1). It is speculated that the peaks at 545 and 612 nm are attributed to the defects, such as zinc interstitial and surface defects, but the accurate reason is unsure at this time. In addition, the small blue-shift between these two samples could be derived from the theory of quantum confinement effect because of the different product feature.

The product of ZnO annealed at 180 °C does not reveal any emission in the measured range (not shown), which indicates the potential to produce a low concentration of oxygen defects and a high optical quality of multicrystal ZnO along with high purity (see the Supporting Information, e.g., the XRD pattern). Uekawa et al. have reported about this.[47]

Conclusion

Stabilized hollow submicrospheres of zinc peroxide (ZnO_2) and zinc oxide (ZnO) were prepared by an environmentally friendly and simple technique. The hollow ZnO_2 submicrosphere preparation method is based on an oxidation procedure by oxygen, with in situ generated gas nanobubbles as a soft template. And the ZnO hollow spheres with the same feature sizes were synthesized by subsequently low-temperature heat treatment. The transformation temperature of ZnO_2 to ZnO was found to be 229 °C by TG-DTA. The use of in situ generated gas bubbles providing aggregation centers is a novel and effective method to fabricate hollow submicro/nanospheres. Compared to the other template synthetic methods, this soft-template method is very simple, convenient, and avoids the introduction of impurities, and is therefore suitable for modern chemical synthesis. This idea might be extended to other solution systems used to synthesize hollow spheres of other metal oxides.

Acknowledgment. We thank YouXiang Li from the Instrument Analysis & Testing Center of Gansu Academy of Science for TEM instrument analysis.

Supporting Information Available: Picture and video of the "explosion procedure" which maintains for several seconds, TGA analysis with different temperature-scan rates, magnified image just at the beginning of decomposition in TG analysis, and PL spectrum of ZnO hollow spheres obtained by heat treatment of ZnO_2 hollow spheres at 180 °C. This material is available free of charge via the Internet at http://pubs.acs.org.

References and Notes

(1) Lou, X. W.; Archer, L. A.; Yang, Z. C. *Adv. Mater.* **2008**, *20* (21), 3987–4019.
(2) Zhong, Z. Y.; Yin, Y. D.; Gates, B.; Xia, Y. N. *Adv. Mater.* **2000**, *12* (3), 206–209.
(3) Li, Z. Y.; Kobayashi, N.; Nishimura, A.; Hasatani, M. *Chem. Eng. Commun.* **2005**, *192* (7), 918–932.
(4) Dinsmore, A. D.; Hsu, M. F.; Nikolaides, M. G.; Marquez, M.; Bausch, A. R.; Weitz, D. A. *Science* **2002**, *298* (5595), 1006–1009.
(5) Liang, H. P.; Zhang, H. M.; Hu, J. S.; Guo, Y. G.; Wan, L. J.; Bai, C. L. *Angew. Chem., Int. Ed.* **2004**, *43* (12), 1540–1543.
(6) Lee, K. T.; Jung, Y. S.; Oh, S. M. *J. Am. Chem. Soc.* **2003**, *125* (19), 5652–5653.
(7) Wang, S.; Xu, H.; Qian, L.; Jia, X.; Wang, J.; Liu, Y.; Tang, W., *J. Solid State Chem.* In press.
(8) Liu, X. M.; Yin, W. D.; Miao, S. B.; Ji, B. M. *Mater. Chem. Phys.* **2009**, *113* (2−3), 518–522.
(9) Teo, J. J.; Chang, Y.; Zeng, H. C. *Langmuir* **2006**, *22* (17), 7369–7377.
(10) Chang, Y.; Teo, J. J.; Zeng, H. C. *Langmuir* **2005**, *21* (3), 1074–1079.
(11) Yu, H. G.; Yu, J. G.; Cheng, B.; Liu, S. W. *Nanotechnology* **2007**, *18* (6), 065604−065611.
(12) Yu, J. G.; Guo, H. T.; Davis, S. A.; Mann, S. *Adv. Funct. Mater.* **2006**, *16* (15), 2035–2041.
(13) Cao, Q. H.; Gao, Y. Q.; Chen, X. Y.; Mu, L.; Yu, W. C.; Qian, Y. T. *Chem. Lett.* **2006**, *35* (2), 178–179.
(14) Lou, X. W.; Wang, Y.; Yuan, C. L.; Lee, J. Y.; Archer, L. A. *Adv. Mater.* **2006**, *18* (17), 2325.
(15) Wang, Y.; Su, F. B.; Lee, J. Y.; Zhao, X. S. *Chem. Mater.* **2006**, *18* (5), 1347–1353.
(16) Park, J.; Shen, X.; Wang, G. *Sens. Actuators, B* **2009**, *136* (2), 494–498.
(17) Zhao, W.; Liu, Y.; Li, H.; Zhang, X. *Mater. Lett.* **2008**, *62* (4−5), 772–774.
(18) Wang, Y.; Zhu, Q. S.; Zhang, H. G. *Chem. Commun.* **2005**, (41), 5231–5233.
(19) Li, B. X.; Rong, G. X.; Xie, Y.; Huang, L. F.; Feng, C. Q. *Inorg. Chem.* **2006**, *45* (16), 6404–6410.
(20) Xu, H. L.; Wang, W. Z.; Zhu, W.; Zhou, L. *Nanotechnology* **2006**, *17* (15), 3649–3654.
(21) Liu, X. Y.; Xi, G. C.; Liu, Y. K.; Xiong, S. L.; Chai, L. L.; Qian, Y. T. *J. Nanosci. Nanotechnol.* **2007**, *7* (12), 4501–4507.
(22) Yu, X. L.; Wang, Y.; Chan, H. L. W.; Cao, C. B. *Microporous Mesoporous Mater.* **2009**, *118* (1−3), 423–426.
(23) Cao, X. B.; Gu, L.; Zhuge, L.; Gao, W. J.; Wang, W. C.; Wu, S. F. *Adv. Funct. Mater.* **2006**, *16* (7), 896–902.
(24) Zhou, H.; Fan, T. X.; Zhang, D. *Microporous Mesoporous Mater.* **2007**, *100* (1−3), 322–327.
(25) Lin, X. X.; Zhu, Y. F.; Shen, W. Z. *J. Phys. Chem. C* **2009**, *113* (5), 1812–1817.
(26) Wang, W. S.; Zhen, L.; Xu, C. Y.; Shao, W. Z. *Cryst. Growth Des.* **2009**, *9* (3), 1558–1568.
(27) Wang, W. S.; Zhen, L.; Xu, C. Y.; Zhang, B. Y.; Shao, W. Z. *J. Phys. Chem. B* **2006**, *110* (46), 23154–23158.
(28) Huang, J. H.; Gao, L. *J. Am. Ceram. Soc.* **2006**, *89* (12), 3877–3880.
(29) Ibarra, L.; Marcos-Fernandez, A.; Alzorriz, M. *Polymer* **2002**, *43* (5), 1649–1655.
(30) Ibarra, L.; Alzorriz, M. *J. Appl. Polym. Sci.* **2002**, *86* (2), 335–340.
(31) Ibarra, L.; Alzorriz, M. *J. Appl. Polym. Sci.* **2002**, *84* (3), 605–615.
(32) Hsu, C. C.; Wu, N. L. *J. Photochem. Photobiol., A* **2005**, *172* (3), 269–274.
(33) Sun, M.; Hao, W.; Wang, C.; Wang, T. *Chem. Phys. Lett.* **2007**, *443* (4−6), 342–346.
(34) Zhang, Y. C.; Wu, X.; Ya Hu, X.; Guo, R. *J. Cryst. Growth* **2005**, *280* (1−2), 250–254.
(35) Rosenthal-Toib, L.; Zohar, K.; Alagem, M.; Tsur, Y. *Chem. Eng. J.* **2008**, *136* (2−3), 425–429.
(36) Chen, W.; Lu, Y. H.; Wang, M.; Kroner, L.; Paul, H.; Fecht, H.-J.; Bednarcik, J.; Stahl, K.; Zhang, Z. L.; Wiedwald, U.; Kaiser, U.; Ziemann, P.; Kikegawa, T.; Wu, C. D.; Jiang, J. Z. *J. Phys. Chem. C* **2009**, *113* (4), 1320–1324.
(37) Pal, E.; Sebok, D.; Hornok, V.; Dekany, I. *J. Colloid Interface Sci.* **2009**, *332* (1), 173–182.
(38) Zhang, Y.; Shi, E. W.; Chen, Z. Z.; Xiao, B. *Mater. Lett.* **2008**, *62* (8−9), 1435–1437.
(39) Li, Z. Q.; Xie, Y.; Xiong, Y. J.; Zhang, R. *New J. Chem.* **2003**, *27* (10), 1518–1521.
(40) Deng, Z.; Chen, M.; Gu, G.; Wu, L. *J. Phys. Chem. B* **2008**, *112* (1), 16–22.
(41) Kou, H.; Wang, J.; Pan, Y.; Guo, J. *Mater. Chem. Phys.* **2006**, *99* (2−3), 325–328.

(42) Zhu, Y. F.; Fan, D. H.; Shen, W. Z. *J. Phys. Chem. C* **2007**, *111* (50), 18629–18635.
(43) Duan, J. X.; Huang, T. X.; Wang, E. K.; Ai, H. H. *Nanotechnology* **2006**, *17*, 1786–1790.
(44) Chen, Z.; Gao, L. *Cryst. Growth Des.* **2008**, *8* (2), 460–464.
(45) Wang, X.; Hu, P.; Fangli, Y.; Yu, L. *J. Phys. Chem. C* **2007**, *111* (18), 6706–6712.
(46) Yu, J. G.; Yu, J. C.; Leung, M. K. P.; Ho, W. K; Cheng, B.; Zhao, X. J.; Zhao, J. C. *J. Catal.* **2003**, *217* (1), 69–78.
(47) Uekawa, N.; Mochizuki, N.; Kajiwara, J.; Mori, F.; Wu, Y. J.; Kakegawa, K. *Phys. Chem. Chem. Phys.* **2003**, *5*, 929–934.
(48) Han, X. F.; Liu, R.; Chen, W. X.; Xu, Z. D. *Thin Solid Films* **2008**, *516* (12), 4025–4029.
(49) Bitenc, M.; Marinsek, M.; Crnjak Orel, Z. *J. Eur. Ceram. Soc.* **2008**, *28* (15), 2915–2921.
(50) Sreekantan, S.; Gee, L. R.; Lockman, Z., *J. Alloy Compd*. In press.
(51) Peng, Q.; Dong, Y. J.; Li, Y. D. *ChemInform* **2003**, *34* (38), 3027–3030.
(52) Yan, C.; Xue, D. *J. Alloy Compd.* **2007**, *431* (1−2), 241–245.
(53) Fan, X.; Zhang, Z.; Li, G.; Rowson, N. A. *Chem. Eng. Sci.* **2004**, *59* (13), 2639–2645.
(54) Lindroos, S.; Leskel, M. *Int. J. Inorg. Mater.* **2000**, *2* (2−3), 197–201.

JP9036028